Inclusive Human Body Modelling for Aerospace Impact Applications

Dipesh Chouhan[1], Jean Bout[1], Qiu-Rui Zai[2], Jia-yi Zhong[2], Galal Mohamed[3]

[1]Arup, UK
[2]Arup, China
[3]Oasys Ltd, UK

Abstract

For dynamic seat certification in the aviation industry, simulation can be a tool leveraged in the design process to assess structural performance and injury criteria of an occupant, prior to physical testing.

Whilst traditionally an anthropomorphic test device (ATD) or virtual ATD (vATD) is used as part of this assessment, the application of human body models (HBMs) in the simulation environment is a growing method of gaining improved insight into biofidelic injury behaviours, providing realism and detail beyond the capabilities of traditional vATDs.

This paper uses Ansys LS-DYNA® simulations of aerospace crash pulses on 50th percentile male and female THUMS HBMs, to understand and demonstrate the dimorphic injury risks between the two models. By leveraging the Oasys LS-DYNA environment, HBMs were positioned appropriately on a simple rigid seat and analysed under two aerospace loadcases. Injury risk between the sexes was identified, quantified and compared.

The results demonstrated good agreement with literature, highlighting increased risk of pelvic fracture, rib injury and alternative kinematics, due to differences with seatbelt interaction and spinal behaviours, for female occupants. Sex specific considerations were also applied to measures of head injury, accounting for differing brain structures.

The application of these methodologies for HBMs, using the Oasys LS-DYNA Environment, have been shown to provide deeper insights into injury mechanics, enhancing the overall understanding of inclusive occupant safety.

Introduction

In the aviation sector, dynamic seat certification requires that crash pulses are applied to an aircraft seat. The structural performance of the seat is then assessed, and injury criteria are evaluated from an anthropomorphic test device (ATD). Finite element analysis can play a crucial part in the design of these seats prior to physical testing, allowing for performance to be predicted from a structural model and injuries extracted from a virtual ATD (vATD), allowing for a more refined final product and improved safety outcomes, at lower expense.

The use of a **T**otal **HU**man **M**odel for **S**afety (THUMS) Human Body Model (HBM), developed by Toyota, in these dynamic seating analyses allows for an enhanced biofidelic view of occupant injury beyond a traditional ATD, by incorporating a detailed model of the human anatomy. These models, shown in Figure 1, contain highly detailed anatomical structures developed from medical imaging, also enabling the implementation of muscle activation, soft tissue damage and realistic spinal behaviours, in addition to a multitude of further injury criteria.

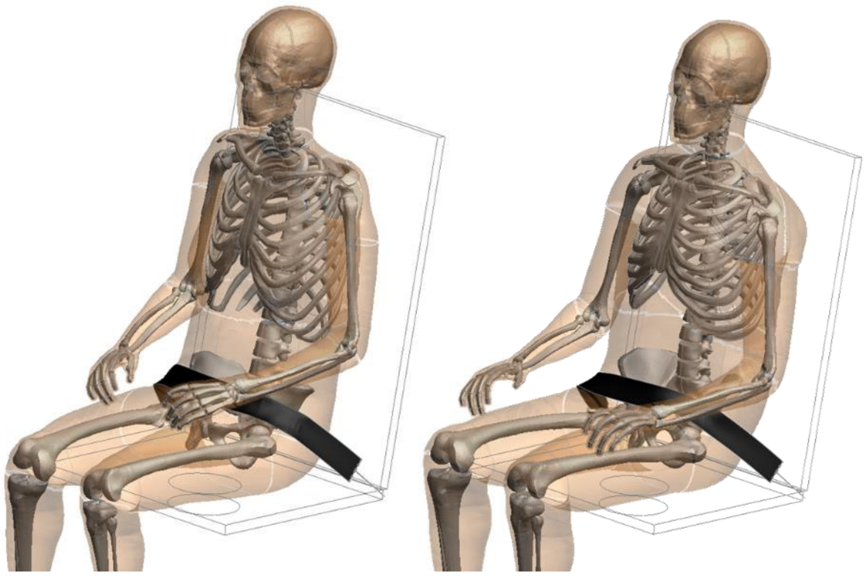

Figure 1 - Image of 50th percentile THUMS HBM for a female (left) and male (right). Internal organs and muscles have been blanked.

This additional nuance in injury assessment is furthered when considering THUMS is available in a variety of physiques, across the sexes. These models account for sexual dimorphism and other key differences in human anthropometry such as fat tissue distribution, bone structure and ranges of motion.

Differences between male and female injury in crash scenarios is the key focus when seeking improved inclusion in occupant safety, aiming to develop safety systems to reduce the bias towards male only testing and consideration in design, to make travel safer for all passengers.

Prior literature has highlighted the need for an adjusted approach when considering female crash occupants, due to the higher injury risks that are presented to them [1].

A notable area of difference relates to the spine and pelvis: the female pelvis is wider, more ovalized, and tilted farther forward than the male pelvis. The bones of the male pelvis are thicker and heavier than those in the female pelvis [2]. These aspects can affect seating position and posture of the occupant in addition to the interaction with the seatbelt during impact; in particular the shape of the female pelvis may cause a “submarining” phenomenon, where the belt rides up onto the abdomen whilst the male pelvis is typically able to better anchor the seatbelt, restraining the occupant as intended.

The female spine differs greatly from the male spine, having a greater degree of curvature (especially in the lumbar vertebra), smaller vertebral cross-sections, lower bone material density and heightened joint laxity [3]. Spinal trauma represents one of the most common forms of severe injury due to highly dynamic events within aviation, highlighting the need for biofidelic representation.

Similarly to spinal trauma, head injury appears as another concern for major injury in reported incidents. Advanced head injury metrics such as BrIC or CSDM are shown to be better measures of risk to Diffuse Axonal Injury (DAI) when compared to HIC [4]. This is especially pertinent when considering that females are reported to demonstrate heightened symptoms, prolonged recovery to mild traumatic brain injury (TBI) and higher likelihoods of TBI linked deaths when compared to aged-matched males [5,6].

Dollé et al [7], highlight the differences in axon structure between females and males, noting that the dimorphism may contribute to more extensive axonal injury in females compared to males exposed to the same mechanical injury. This suggests that even advanced metrics that pertain to DAI should consider using altered damage thresholds to account for this difference.

There also exists a clear degree of dimorphism between the ribs of males and females. Males tend to have a more voluminous ribcage whilst also having a shorter section of ribs, resulting in a stiffer ribcage. The lower ribs also exhibit more lateral protrusion than seen in females. Conversely, female ribs tend to have a pronounced downward inclination, with a shorter and thinner sternum compared to males, resulting in a more compliant ribcage.

Figure 2 below highlights the ribs and sternum of the AF50 and AM50 THUMS models, which demonstrate the differences in anatomy.

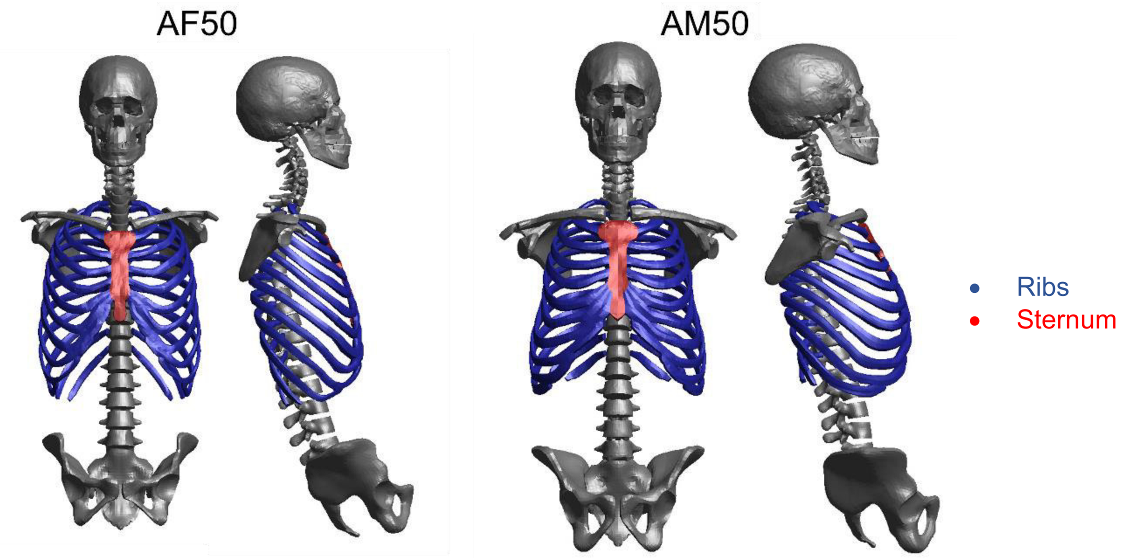

Figure 2 - Image of THUMS HBM showing the ribs and sternum for a female (left) and male (right). Organs and muscles have been blanked.

Despite the clear indication within literature of the potentially greater risk of injury for females, there currently exists a general lack of sufficient representation for females in respect to safety testing within the aviation industry. Official regulations often only require testing to be conducted using male representative ATDs. When female ATDs are utilised, often a female 5th percentile ATD will be used, which will inevitably not be representative of most of the female population. Furthermore, when considering HBMs, the 50th percentile female occupant model (AF50) has only recently become available, in the Version 7.1 series release of the THUMS HBMs.

Therefore, it was decided for this study to use the latest (Version 7.1) male (AM50) and female (AF50) 50th percentile THUMS HBMs, to compare the injury risks between the two sexes.

The entire modelling workflow was achieved using the Oasys LS-DYNA Environment and Ansys LS-DYNA®, as will be discussed.

Simulation Based Positioning of HBMs

Simulation-based positioning (SBP) for each HBM model was used to accurately place the model into position. This was achieved with the aid of pre-configured tree files for THUMS, allowing each region of the occupant to be appropriately articulated into the target position.

Once target positions were defined in Oasys PRIMER, up to three cables were automatically created and attached to stiff components (bone structure) of each assembly of the HBM. This model was then run in a LS-DYNA positioning analysis, where the cables shrank to zero length, essentially 'pulling' the limbs of the HBM into the desired position. Post-processing checks were then undertaken to assess element quality and initial penetrations.

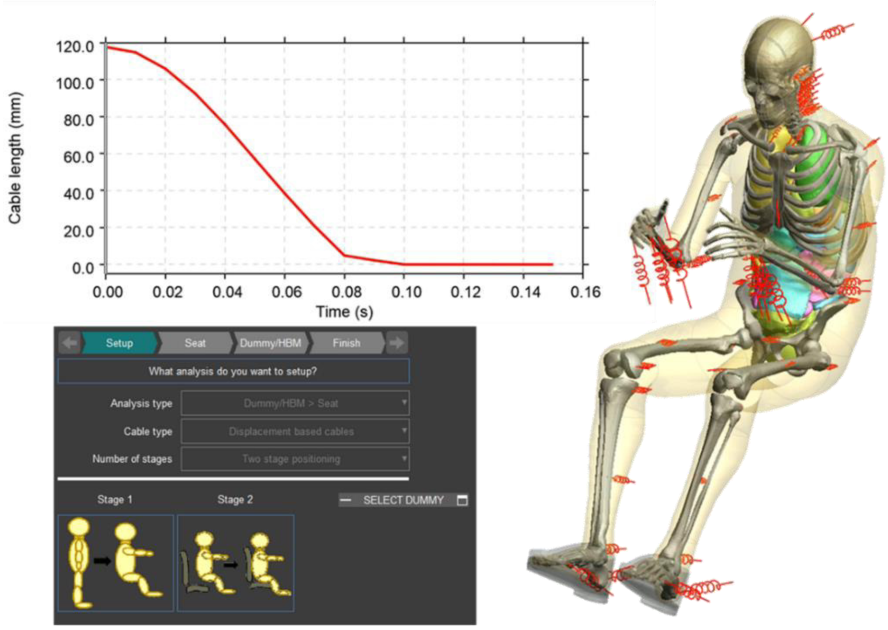

Figure 3 - Overview of HBM Simulation Based Positioning using Oasys PRIMER.

For this study, each HBM was positioned onto a simplified rigid seat, to establish a similar relative posture, derived from actual ATD postures from physical dynamic tests. A 2-point seatbelt was also fitted around the laps of the HBMs, using the Oasys PRIMER Seatbelt Fitting tool, adopting material properties calibrated from physical test data [8].

Once positioned, the HBMs underwent a dynamic relaxation analysis where a 1g load was applied in the vertical direction, emulating settling due to gravity. Force Transducer contacts between the HBM, the ground and rigid seat were implemented to conduct post-processing force equilibrium checks, ensuring convergence had been reached and the model was in a settled state. The deformed HBM nodal coordinates were then used as input into the main dynamic analysis.

The models used in this study (AF50 and AM50) were used with 2 levels of muscle activation, sleeping (no activation) and normal. The 'no activation' muscle condition simulates the muscles in a completely relaxed and passive state, with no resistance to external forces from muscular tension. In the 'normal activation' muscle condition, the muscles are actively engaged to maintain posture and respond to external stimuli, simulating a conscious and alert human. For further details please refer to the THUMs manual documentation.

The heights and weights of the two HBMs are included in Table 1.

It is important to note that the THUMS models did not have bone fracture/material erosion enabled, in order to produce stable model outputs. This limitation must be considered upon review of results.

Table 1 - Overview of Occupant types and properties

Occupant Type	Height (cm)	Weight (kg)
Male 50th Percentile (AM50)	179	78
Female 50th Percentile (AF50)	162	62

Loadcase Overview

This study reviews two dynamic seating test cases specified by FAA Title 14 CFR 25.562 & 23.562. The two crash pulses prescribed for seat certification sled tests are described in Table 2:

Table 2 - Summary of Dynamic Seating Cases

Orientation	Pulse Magnitude (g)	Seat Type	Crash Pulse
Horizontal 0 deg	16	Rigid	25.562
Vertical 60 deg	19	Rigid	23.562

The horizontal pulse has a peak acceleration of 16g. This test configuration is used to evaluate head path, pelvis kinematics, and belt forces.

The vertical 60-degree pitch condition has a peak acceleration of 19g. The main purpose of this test is to evaluate the lumbar force.

Both loadcases use a two-point seatbelt to restrain the occupant. All analyses were run for approximately 300ms (0.3s). The acceleration pulse shape was a symmetrical isosceles triangle, seen in Figure 4. The regulations [9] prescribe the use of either the Hybrid II or FAA Hybrid III ATD, with straight lumbar spines, however for this study, the loadcases were conducted using the THUMS Version 7.1 AF50 and AM50 HBMs.

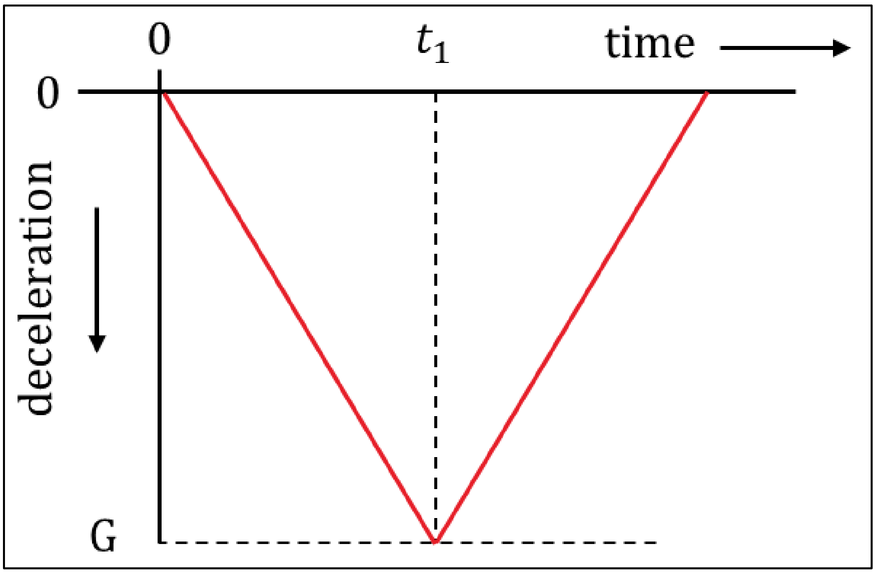

Figure 4 - Illustration of the isosceles acceleration pulse applied across each dynamic case, the peak G varying between cases.

Horizontal Pulse Results

Kinematics Overview

Evaluating the 16g horizontal case, both HBMs followed a similar kinematic pattern through the application of the pulse, shown in Figure 55. Both HBMs underwent a forward movement relative to their seats, with the pelvises engaging the 2-point belt. Between 0.1-0.2s, the upper bodies of both HBMs rotated around the seatbelt; the AF50 demonstrated greater elongation of the spine as well as slipping of the belt down towards the acetabulum. The male head collided with the legs, whilst the female head ultimately ended up striking the forward portion of the seat, seen at 0.3s (end of analysis).

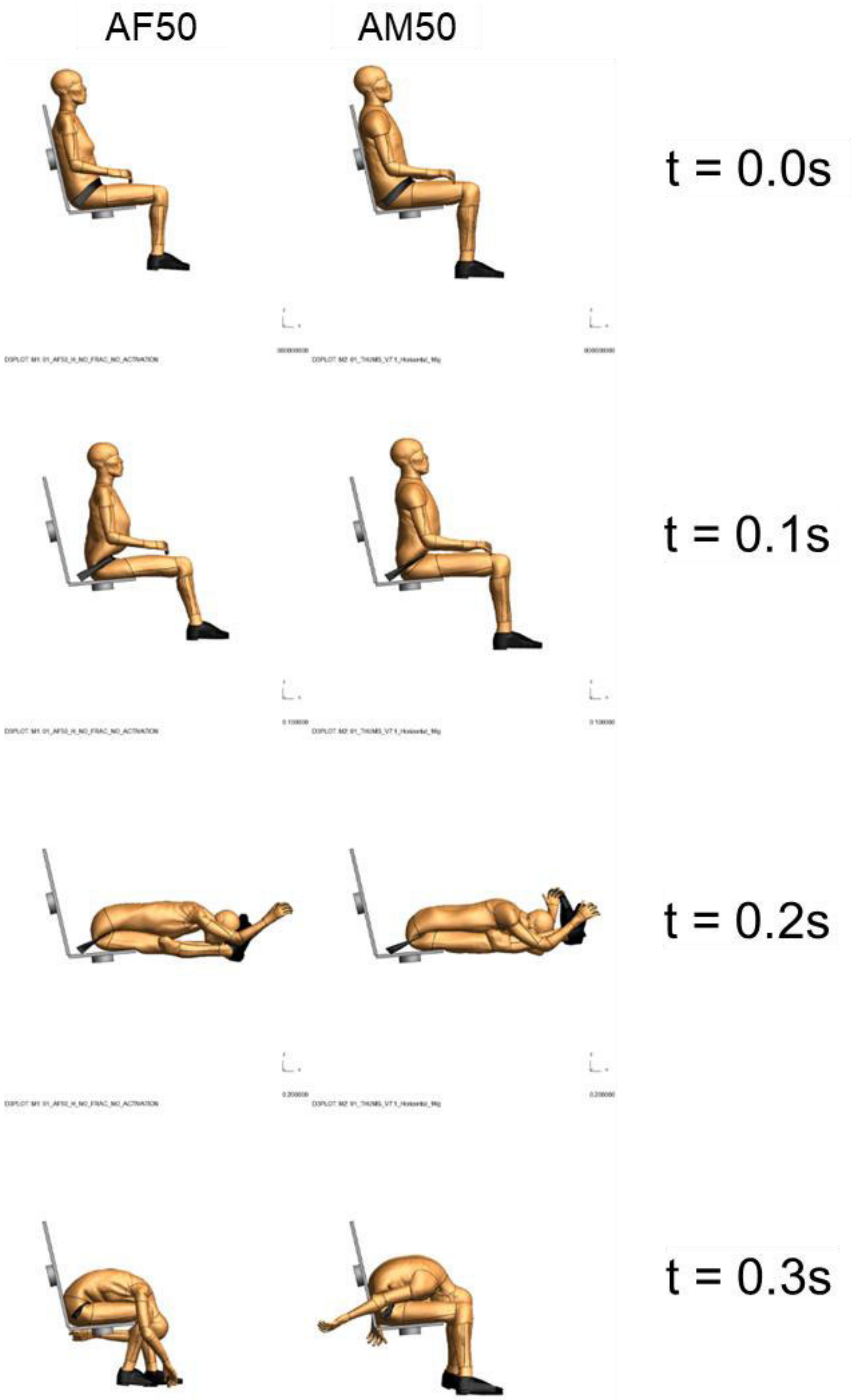

Figure 5 - Comparison of AF50 to AM50 ('no' activation) horizontal pulse kinematics.

The differences in spinal and pelvis behaviour are further evident in Figure 6, where the key structures have been isolated using Oasys D3PLOT. The pelvis of the female was seen to undergo a greater extent of rotation, enabled by the aforementioned belt slip. The increased vertebral laxity in the female spine, especially prominent in the lumbar and cervical spine, compounded upon the pelvic rotation, causing differences in head trajectories.

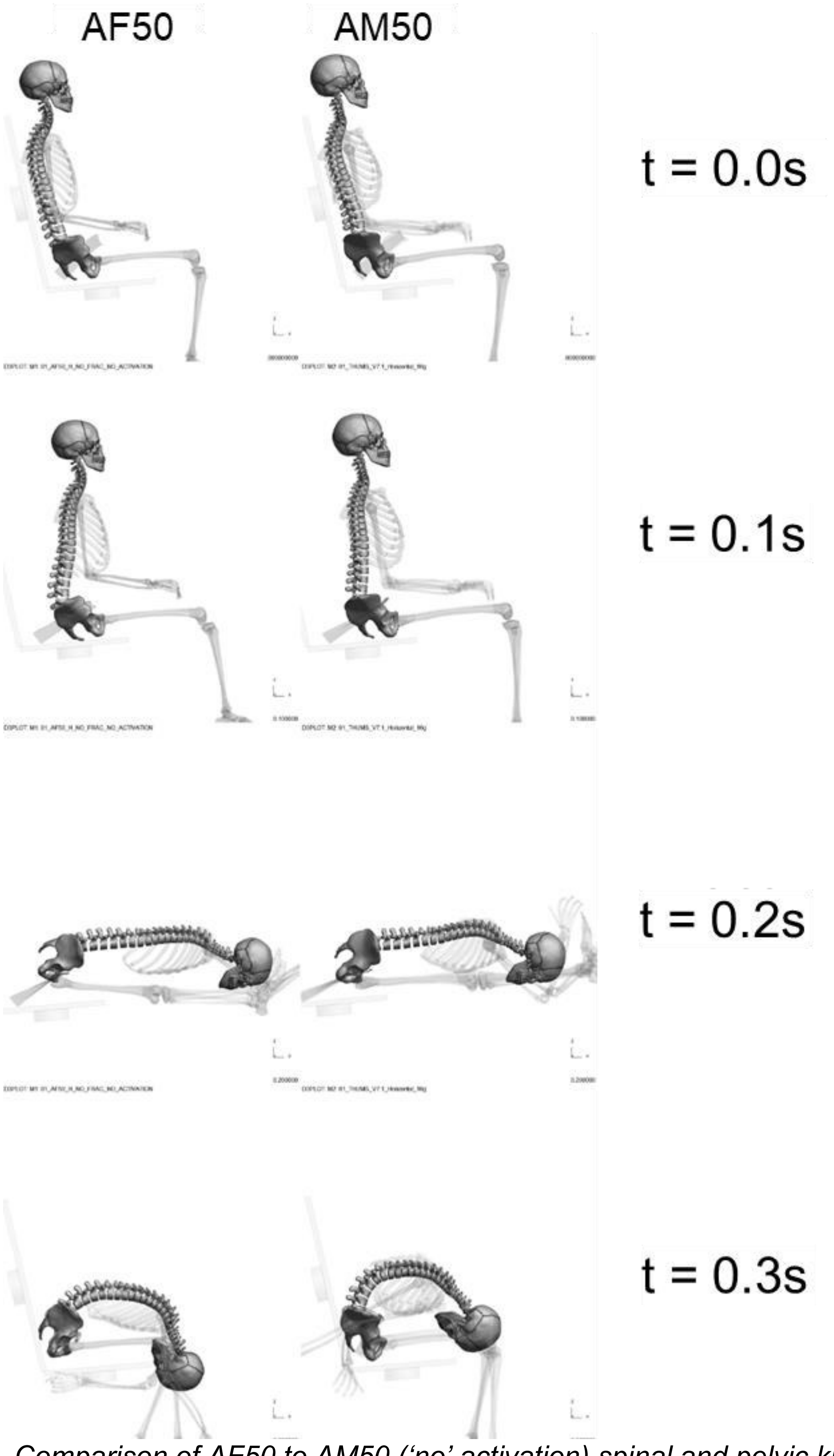

Figure 6 - Comparison of AF50 to AM50 (‘no’ activation) spinal and pelvic kinematics.

The downstream effects of this behaviour can be observed in Figure 7, which shows the trajectory of both the AF50 and AM50 heads, for both levels of muscle activation. This was determined by plotting the trace of the centre of gravity (CoG) of each models' head, using Oasys T-HIS.

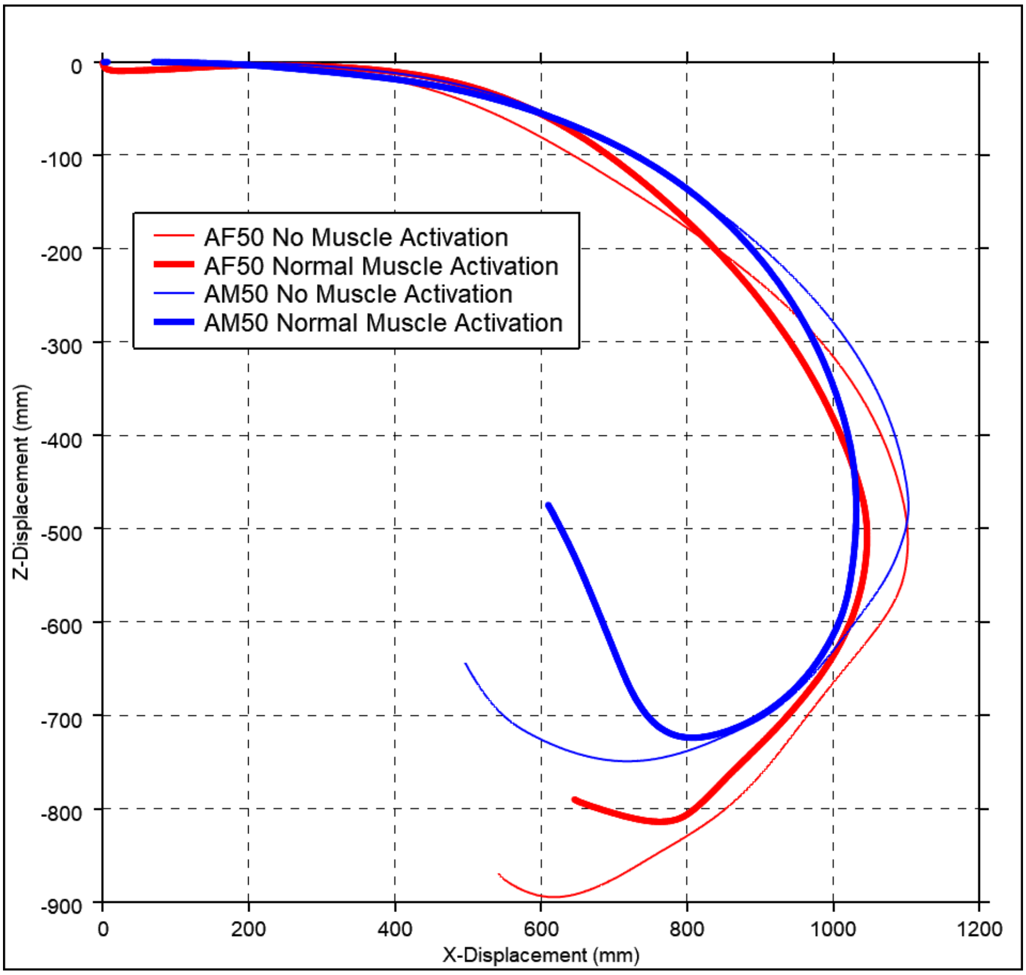

Figure 7 - Comparison of head CoG trajectories between AF50 and AM50 between 'No' and 'Normal' muscle activation.

Comparing trajectories, the female head underwent a similar amount of x-displacement as the male for both activations, despite the shorter spinal length. The female demonstrated between 100-150 mm of additional z-displacement compared to its equivalent level of muscle activation, facilitated by the previously described kinematics.

The difference between each sex is also apparent when reviewing muscle activation. Whilst both HBMs travelled a shorter path with "normal" muscle activation, the female occupant demonstrated a smaller delta in the final head position between the two levels of muscle activation when compared to the male. This highlights how the reduced extent of muscle mass for the female model limited the occupant's ability to control the motion of the neck and head during impact.

For both HBMs, the resulting behaviours seen between the two levels of muscle activation were relatively similar, therefore, only "no muscle activation" results and injury metrics are reported henceforth, for the benefit of clarity and conciseness.

Pelvic Injury

Reviewing pelvic and femur injury in greater detail, the principal strains near the femoral head and neck are visualised in Figure 8.

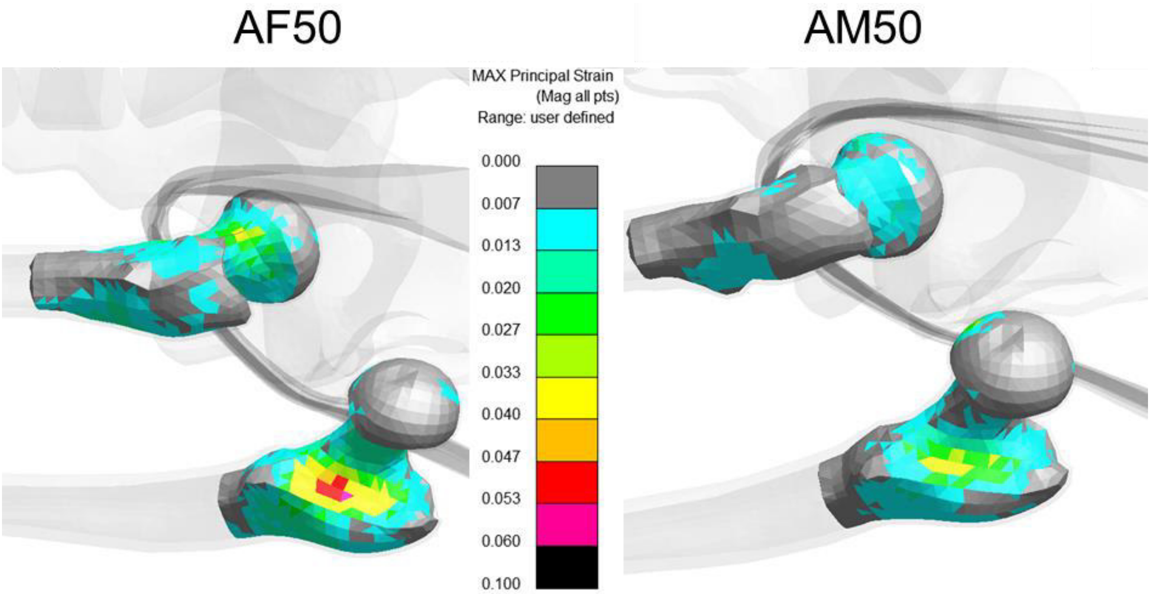

Figure 8 - Comparison of Femoral strains applying a strain threshold of 6%.

As previously mentioned, bone fracture/material erosion was disabled during the analyses conducted for this study, but the strain failure limits utilised by the THUMS model with fracture properties enabled are used in the strain contours seen above, to indicate locations at greatest risk of fracture. The THUMS model specifies a 6% failure strain for the femoral head/neck region for both the AF50 and AM50 models.

The elements in black in Figure 8 represent elements exceeding this failure strain value. The female HBM demonstrated strains that approach this 6% limit, whereas the male HBM exhibited a similar utilisation pattern but a lower magnitude of strain.

Assessing risks to pelvic fracture, Figure 9 shows a strain contour plot for the AF50 and AM50 pelvises. Elements exceeding the bone failure strain threshold are shown in black. Both HBMs developed strains above the cortical bone strain thresholds defined by the THUMS bone fracture model, using data provided by [10]. This suggests that both pelvises could be at risk of developing fractures.

The belt forces for each pelvis are shown in Table 3, highlighting how both models experienced a broadly similar force of restraint (once normalised for bodyweight).

Table 3 - Occupant Belt Forces (Averaged from left and right points)

Occupant	AF50	AM50
Belt Force (N)	7350	8690
Multiple of Bodyweight	12.00	11.35

Observing the male pelvis, the area above the strain threshold was located predominantly in the anterior iliac region, where the seatbelt interfaces. The AM50 also exceeded the strain threshold on the caudal region of the acetabulum. The AM50 model demonstrated limited posterior strain threshold exceedance.

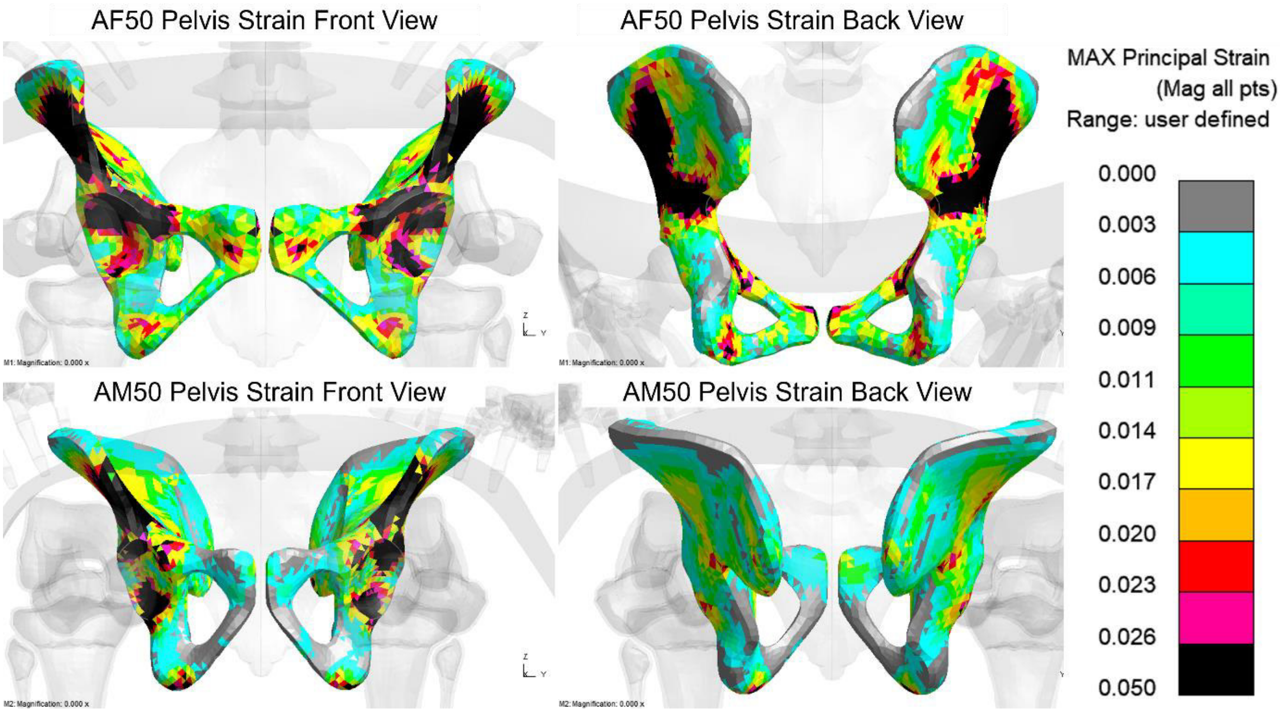

Figure 9 - Overview of Pelvic Max Principal Strain between each sex.

The AF50 in comparison had a far greater extent of strain exceedance than the AM50. The strains near the anterior iliac region propagated posteriorly to the rest of the wing of the ilium. Strain exceedances of the acetabulum were generally more cranially located than in the AM50. Whilst this model does not include fracture properties for the bone, the significant extent of strain exceedance on the AF50 suggests a higher risk compared to the male occupant.

Head Injury

Comparing head injury across the two occupants, the cumulative strain damage measure (CSDM) was measured by calculating the instantaneous CSDM value at each time step. This was determined by dividing the volume of elements that exceeded the strain damage threshold by the total volume of solid brain elements.

This was calculated by implementing a JavaScript in Oasys D3PLOT and Oasys T-HIS. Figure 10 shows an example of a strain plot for the AF50 model, indicating brain damage, at one state during the analysis.

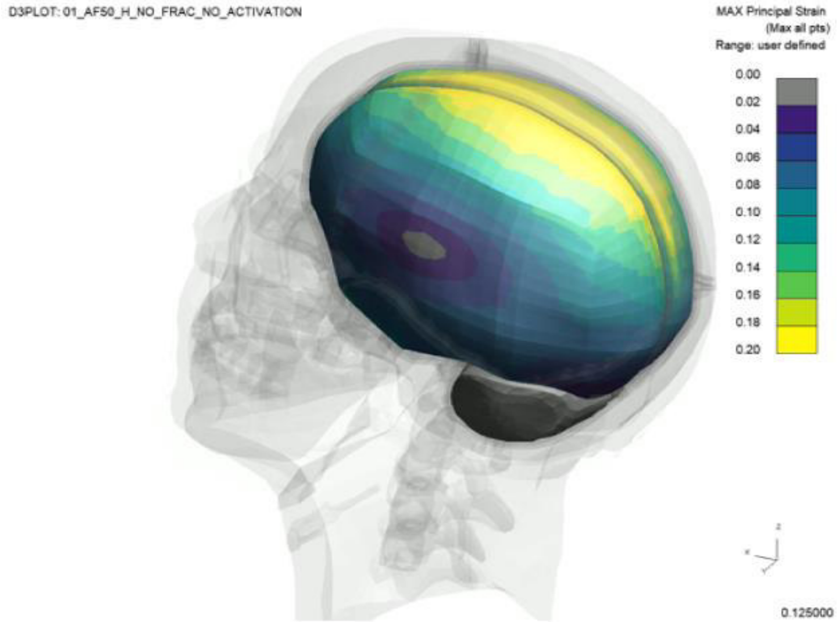

Figure 10 - Brain strain contour plot for AF50 model (image taken at one time state during analysis for illustrative purposes).

Thresholds for strain correlated to DAI are often cited between 0.15 - 0.25. Initially, the same strain damage threshold of 0.25 was selected for both the AF50 and AM50 models. This resulted in a lower CSDM value for the female occupant, indicating reduced brain damage. However, Dollé et al suggested that differences in axonal structure between males and females predispose females to increased pathology for the same mechanical input. Therefore, a lower strain threshold was subsequently utilised for the female occupant in the CSDM calculation. Table 4 highlights these results.

Table 4 - Comparison of CSDM, applying modified thresholds for each occupant.

Occupant	AF50	AM50
Max Principal Strain Threshold	0.25	0.25
CSDM	0.50	0.69
Adjusted Max Principal Strain Threshold (AF50 Only)	0.20	0.25
Adjusted CSDM	0.71	0.69

The authors of this paper selected a new strain threshold of 0.2 to accommodate the increased sensitivity of the female (compared to 0.25 for the male). Whilst the applicability of this value and determination of an appropriate difference in threshold stands as a topic for future investigation, the authors aim to highlight how a differing approach may be required in order to facilitate equitable design across the sexes.

Rib Injuries

As previously mentioned, bone fracture (element erosion) was not enabled during the analyses, in order to produce stable model outputs. Therefore, a probabilistic approach to rib injury was employed.

A strain threshold of 2%, commonly agreed upon in literature [11,12], was utilised as the failure limit for the ribs, for both models. Figure 11 shows a plastic strain contour plot of the AF50 and AM50 ribs, where the black elements represent exceedance of this failure strain, thus indicating rib fracture.

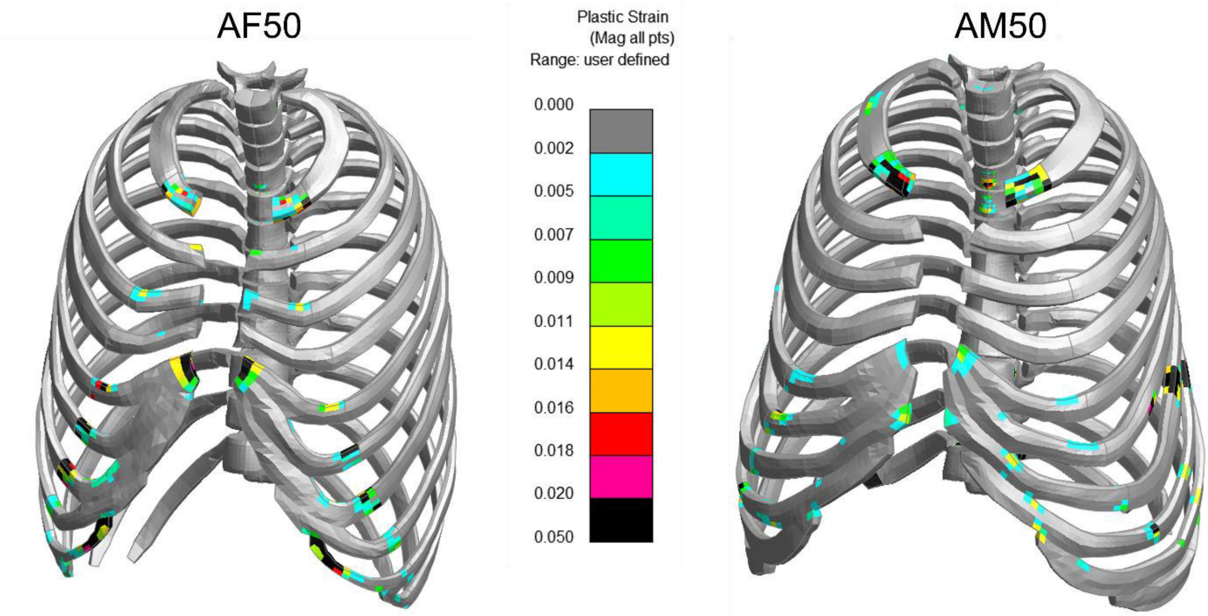

Figure 11 - Overview of Ribcage Plastic Strain for each sex.

As shown, there are clear differences in the strain patterns between the male and female ribs. The AF50 model saw the highest strains anteriorly, due to the impact of the ribs against the legs. This resulted in a higher number of locations of strain failure exceedance, when compared to the AM50 model, which, conversely, saw the highest strains laterally, predominantly on the lower ribs.

These results agree with literature, as the higher occurrence of elements exceeding the failure strain in the AF50 ribs, indicated that the female ribcage was generally more compliant than the male ribcage. The stiffer ribcage of the male, as well as the slight lateral protrusion of the male's lower ribs, explain the indicative fracture locations seen laterally on the AM50 ribcage.

Literature suggests that having more than 6 ribs fractured corresponds to an AIS 3+ injury [11,12]. This would suggest that females have a higher likelihood of serious injury, with more fracture locations identified for the AF50 model. However, the AM50 model experienced more lateral rib fracture which may be considered a more severe injury, due to the proximity of internal organs, particularly the liver and spleen, which may be at risk of puncture or laceration by fractured ribs.

It is important to note, that because element erosion was disabled, stress redistribution and the domino effects of rib fracture [11] were not captured in the analyses. Nevertheless, the clear differences in injury risk and location between the AF50 and AM50 models corroborate with literature.

Vertical Pulse Results

The 19g 60 degree pitched case is used to evaluate spinal injury upon impact. Both HBMs followed a similar kinematic pattern from the acceleration pulse, shown in Figure . Both HBMs underwent a downward movement into their seats, with each pelvis sliding forwards upon the application of the acceleration pulse. Their heads and necks initially underwent extension before transitioning to flexion between 0.1s-0.2s. This behaviour was driven by spinal compression between 0.0s-0.1s.

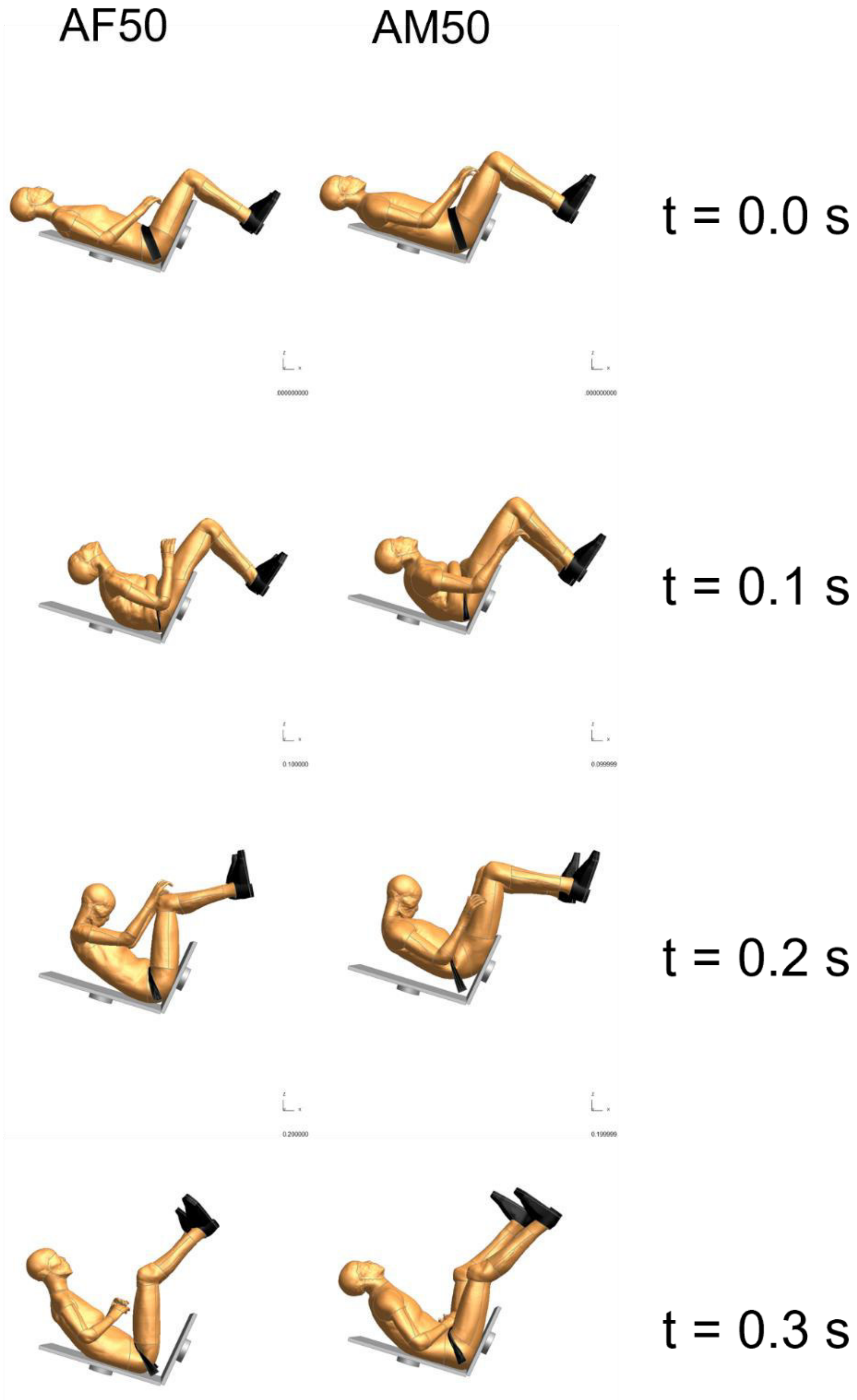

Figure 12 - Comparison of AF50 to AM50 (‘no’ activation) vertical pulse kinematics.

Isolating the sketetal structures in Figure 13 , the key differences in the spinal response between the two HBMs are highlighted. A greater extent of spinal curvature was seen for the female occupant, promoted by increased spinal flexabilty. The female cervical spine also appeared to undergo a greater degree of flexion and extension versus the male. The pelvis of the female was also seen lifting up out beyond the seat, to a greater extent than the male.

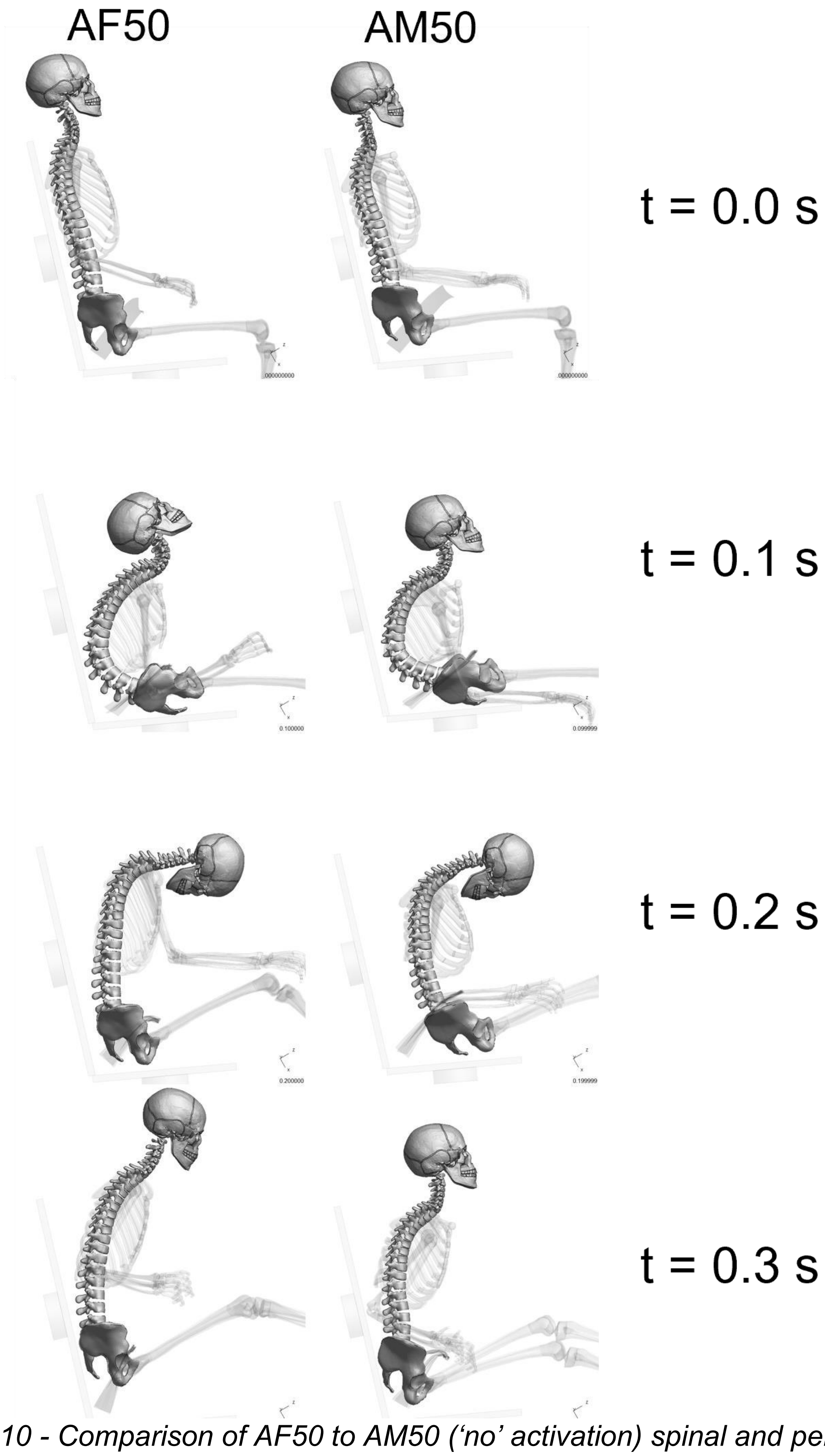

Figure 10 - Comparison of AF50 to AM50 ('no' activation) spinal and pelvic vertical kinematics.

Assessing the risk to vertebral damge, Figure 14 plots the strain of the vertebra using a strain threshold of 1%, balancing the strain limits of the porous trabecular bone and denser cortical bone that form the vertebra. We can see both spines developed regions above this threshold, in line with risk to fracture types, such as compression, wedge and burst. These strains were most prevalent in the anterior region of the lumbar spine. The AF50 had strain develop reasonably evenly across the anterior region across the thoracolumbar region. The less flexible lumbar spine of the AM50 concentrated these strains across the lumbar vertebra over a greater volume of the vertebra.

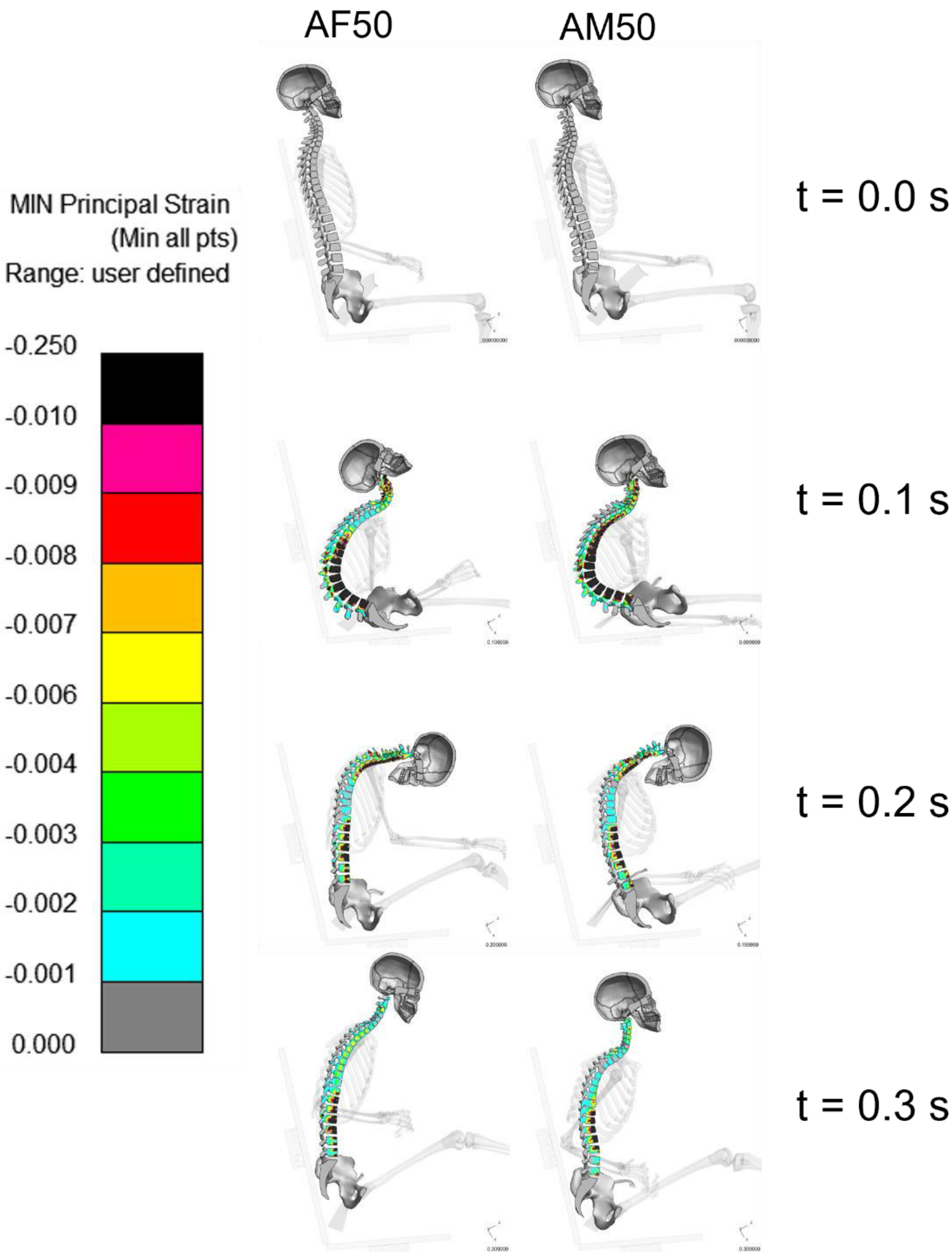

Figure 11 – Cut-section contour plot comparing compressive strain in spines of AF50 and AM50 models.

The AM50 spinal shape is highlighted in Figure 15, with far less gradual curvature than the female and pronounced differences in vertebral articulation at the thoracolumbar junction (T12-L2) .

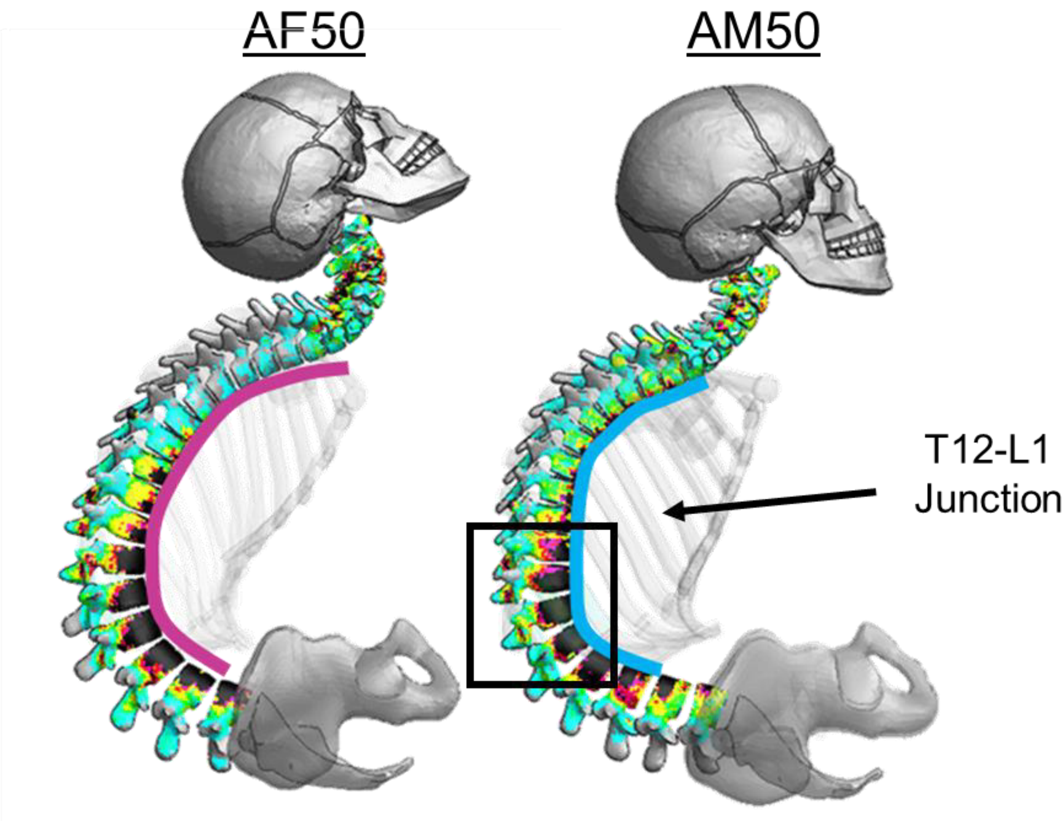

Figure 12

FAA regulation only requires the lumbar load to be below 6672N (1500lbs) [9], however this is solely based upon testing of Hybrid II Male ATDs, with no consideration for other sized occupants. Both occupants in this study achieved loads below this threshold, shown below in Table 5.

Although the AF50 model had a lower peak compressive lumbar load than the AM50, normalising these values to their respective weights, the AF50 lumbar load was approximately 11% greater than the AM50, highlighting the increased risk of serious spinal injury for females in vertical impacts.

Table 5 - Comparison of peak lumbar compression force, averaged over lumbar spine.

Occupant	AF50	AM50
Averaged Peak Lumbar Force (N)	3520	3970
Multiple of Bodyweight	5.8	5.2

Summary and Next Steps

An evaluation of two HBMs was successfully undertaken using the Oasys LS-DYNA Environment for two aerospace loadcases. Different risks between sex and occupant anthropometries were identified, highlighting the applicability of HBMs for enabling inclusive safety design by providing enhanced insight into injury risks.

It was found that in the horizontal certification case for a rigid seat, an AF50 HBM experiences an increased degree of strain across a greater extent of the pelvis compared to a male, potentially increasing the risk of pelvis/hip fracture. Both models exhibited high strains at locations highlighted as being at greatest risk of fracture in literature. The pelvis for the female occupant also showed a higher amount of rotation when compared to the AM50. This additional rotation, in combination with the differences in the spine, allowed the female HBM head trajectory to follow a longer path than the male. This highlights the risk associated with collision in areas of the cabin interior.

When considering head injury, differing approaches to CSDM were utilised to account for dimorphism in axon structure for DAI, bringing female head injury severity approximately in line with male injury risk, for this study. Rib fracture risk was compared across both HBMs, finding that the stiffer rib cage of the AM50 developed higher fracture risks in the lateral region whereas the AF50's rib injuries were more anteriorly located.

In the vertical certification case, spinal behaviours under compression were evaluated. It was found that the female experiences ~11% higher lumbar compression loads relative to bodyweight than the male. The female spine displayed a greater extent of flexibility compared to the male upon impact.

The male spine exhibited a clear example of thoracolumbar vulnerability in its deformed shaped upon impact. Both spines achieved compressive strains above the threshold for vertebral trabecular bone failure and close to cortical bone strain limits, highlighting the risk of potentially severe spinal injury. This was especially prominent when reviewing the AF50 cervical spinal strain.

This study makes evident the clear differences in injury risk between female and male occupants. Further empirical work would be beneficial in verifying the results produced by this study, as test data for females is generally lacking within literature.

Future work on this topic will focus upon the following areas:

- Review of other sizes of HBM for a more comprehensive overview of injury risk across morphologies, (AF05, AM95, pregnant, obese or child occupants).
- Incorporation of more realistic seating structures and seating arrangements (groups of seating rows together).
- Wider range of occupant postures in accordance with civil aviation standards.
- Inclusion of other industry-leading HBMs.

Literature

[1] Liu, C., Subramanian, R. The Relationship Between Passenger Vehicle Occupant Injury Outcomes and Vehicle Age or Model Year in Police-Reported Crashes. Traffic Safety Facts Research Note: Report No. DOT HS 812 937). National Highway Traffic Safety Administration. 2020.

[2] Arregui-Dalmases, C., Kerrigan, J. R., Sanchez-Molina, D., Velazquez-Ameijide, J., & Crandall, J. R. A Review of Pelvic Fractures in Adult Pedestrians: Experimental Studies Involving PMHS Used to Determine Injury Criteria for Pedestrian Dummies and Component Test Procedures. Traffic Injury Prevention Vol 16(1), pp 62-69. 2014.

[3] Mohan, M., Huynh, L. Sex Differences in the Spine. Current Physical Medicine and Rehabilitation Vol 7, pp 246-252. (2019).

[4] Takhounts, E. G., Craig, M. J., Moorhouse, K., et al. Development of Brain Injury Criteria (BrIC). Stapp Car Crash Journal Vol 57, pp 243-266. 2013.

[5] Valera, E. M., Joseph, A. L. C., Snedaker, K., et al. Understanding Traumatic Brain Injury in Females: A State-of-the-Art Summary and Future Directions. Journal of Head Trauma Rehabilitation Vol 36(1), pp 1-17. 2021.

[6] Colantonio, A., Harris, J. E., Ratcliff, G., et al. Gender Differences in Self Reported Long Term Outcomes Following Moderate to Severe Traumatic Brain Injury. BMC Neurology Vol 10. 2010.

[7] Dollé, J. P., Jaye, A., Anderson, S. A., et al. Newfound Sex Differences in Axonal Structure Underlie Differential Outcomes from In Vitro Traumatic Axonal Injury. Experimental Neurology Vol 300, pp 121-134. 2018.

[8] Gerardo, O. Hybrid II and Federal Aviation Administration Hybrid III Anthropomorphic Test Dummy Dynamic Evaluation Test Series. DOT/FAA/AR-11/2. 2013.

[9] Federal Aviation Administration. Emergency landing dynamic conditions, Title 14 Code of Federal Regulations 25.562, U.S. Government Publishing Office. 2025. [Online]. Available: https://www.ecfr.gov/current/title-14/chapter-I/subchapter-C/part-25/subpart-C/subject-group-ECFRda24a9b1d389632/section-25.562

[10] Yamada, H. Strength of Biological Materials. Robert E. Krieger Publishing Co Inc, NY USA. 1973.

[11] Song, E., Lecuyer, E., Trosseille, X. Development of Injury Criteria for Frontal Impact Using a Human Body FE Model. 22nd International Technical Conference on the Enhanced Safety of Vehicles 2011.

[12] Petitjean, A., Baudrit, P., Trosseille, X. Thoracic Injury Criterion for Frontal Crash Applicable to All Restraint Systems. Stapp Car Crash Journal Vol 47, pp 323-348. 2003.